WILEY | Hindawi

Research Article

Design a Compact and Miniaturized Unit Cell in Substrate Integrated Plasmonic Waveguides

Salma Mirhadi ⓘ,[1] Zahra Javidi ⓘ,[2] and Nader Komjani ⓘ[2]

[1]Department of Electrical and Computer Engineering, Technical and Vocational University, Tehran, Iran
[2]Electrical Engineering Department, Iran University of Science and Technology, Tehran, Iran

Correspondence should be addressed to Salma Mirhadi; s.mirhadi@shariaty.ac.ir

This paper presents a novel procedure to design a compact and miniaturized unit cell in the substrate integrated plasmonic waveguide (SIPW) structures. The slot of the unit cell is automatically obtained in this method without needing any prior knowledge of its shape. The method is based on topology optimization through pixelization of the slot surface in the unit cell and uses a combination of binary particle swarm optimization (BPSO) and commercial electromagnetic (EM) software. With this method, first, the shapes of the two unit cells are engineered to arbitrarily reduce the high cut-off frequency. Then, two low-pass filters consisting of the proposed unit cells are designed and simulated. To further verify the proposed procedure, one of the filters is fabricated, whose measurement results are in good agreement with the simulation results. This filter provides a pass band of 5.6 to 6.3 GHz and has dimensions of $0.82\lambda_g \times 0.22\lambda_g$. The proposed method has the potential to minimize microwave and terahertz devices.

1. Introduction

Substrate integrated plasmonic waveguides (SIPWs) which have attracted attention in recent years are formed by etching slots on metal layers of the substrate integrated waveguide (SIW) to support the spoof surface plasmon polaritons (SSPP) mode at microwave and terahertz (THz) frequencies [1–19]. The SIPW inherits the characteristics of both SIW and SSPP and exhibits bandpass behavior; its low cut-off frequency depends on the width of the SIW, and its high cut-off frequency can be individually adjusted with the shape and the dimension of the slots. Simple rectangular-shaped and comb-shaped slots have first been proposed in [1–11]. However, to reduce the high cut-off frequency and design more compact microwave and THz devices, the length of slots has to be longer. It is possible to extend the slots transversely up to a certain limit due to the finite width of the SIW. In addition, the longer the slots, the more difficult the impedance matching. Therefore, different slot shapes have been proposed whose asymptotic frequency is lower than that of the traditional

rectangle slot. Dumbbell-shaped and T-shaped slots have been presented in [12–15], respectively, and have better field confinement than the traditional rectangle-shaped slot. Furthermore, an on-chip terahertz SIW filter with the Yagi-Uda antenna-like slots has been proposed in [16] which effectively reduces asymptotic frequency compared to previous structures. Asymptotic frequency reduction using meander slot on SIW is also shown in [17]. In [18], a compact bandpass filter with a fishbone-shaped and hourglass-shaped slot has been designed with better electromagnetic (EM) field confinement than that of the comb-shaped slot.

In this paper, we introduce a new procedure to design the slot shape of a SIPW unit cell automatically. Unlike previous traditional methods in which the predetermined shape of the unit cell is applied and its dispersion curve is controlled by varying geometrical parameters, this novel method is based on slot shape extraction with a connection between the binary particle swarm optimization (BPSO) algorithm and a full-wave EM simulator. This procedure has the advantage of designing the SIPW unit cell with the
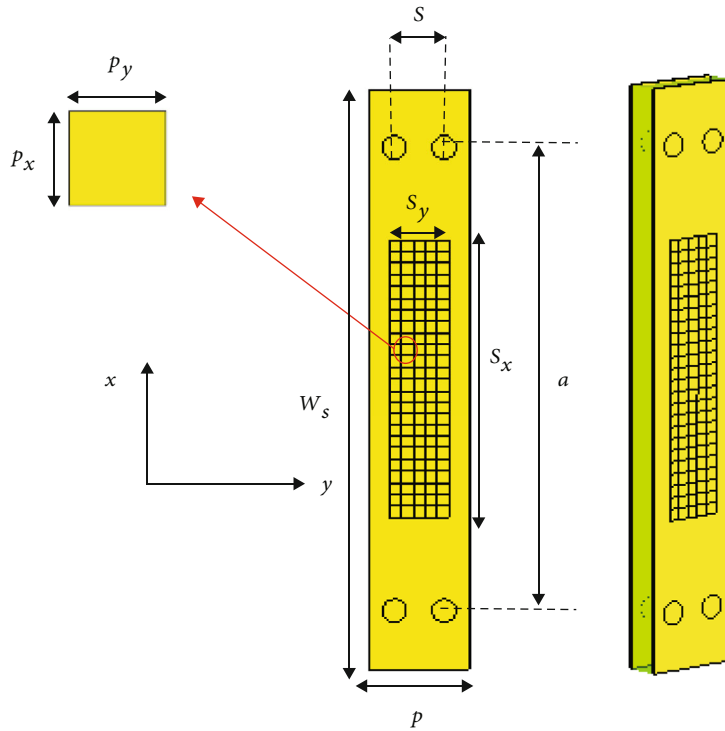
FIGURE 1: The SIPW unit cell under optimization. Yellow and green indicate metal and substrate, respectively.
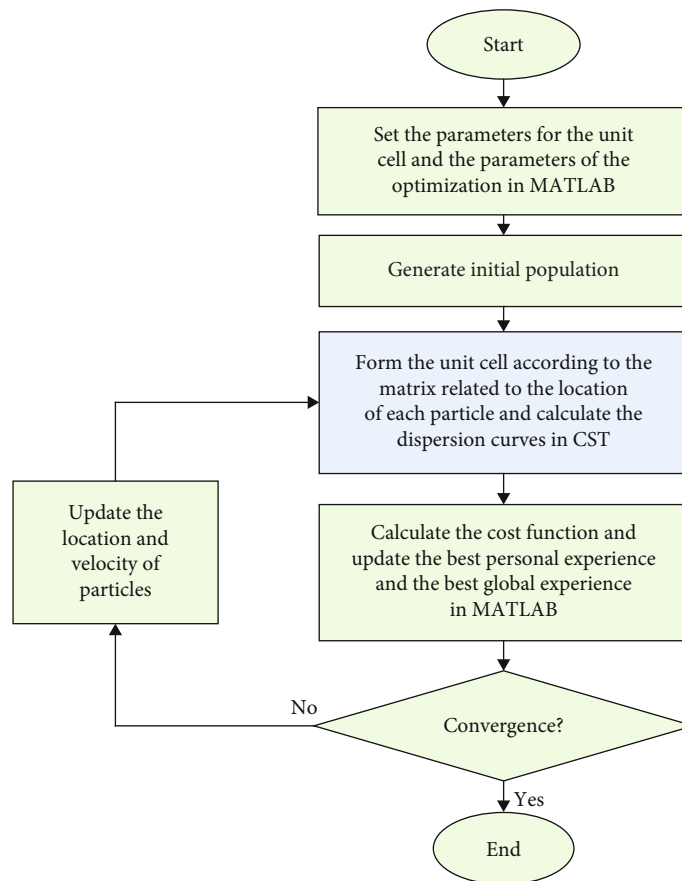

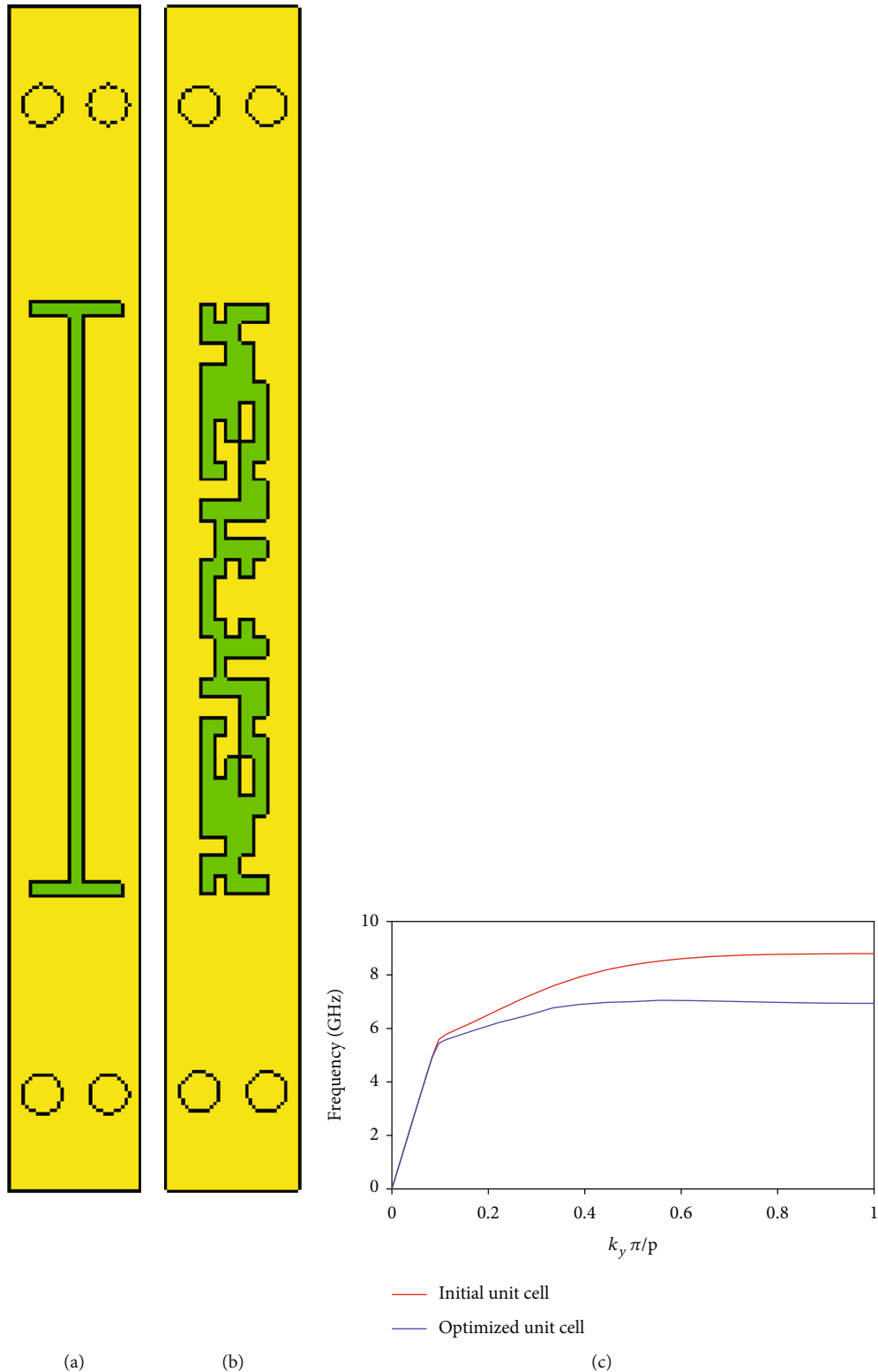FIGURE 2: The flowchart of the optimization process.

FIGURE 3: (a) Schematic configuration of the initial unit cell in the first design. (b) Schematic configuration of the optimized unit cell in the first design. (c) Dispersion curves of the unit cells in the first design. The parameters are selected as (in mm) $p = 2$, $p_x = 0.3$, $p_y = 0.2$, $a = 15$, $w_s = 18$, $s = 1$, $S_x = 9$, and $S_y = 1$.

desired reduction at asymptotic frequency to achieve strong field confinement. First, the design procedure is discussed, and then, two SIPW unit cells with different values of asymptotic frequencies are achieved. Finally, to verify the proposed method, a SIPW waveguide prototype of the proposed unit cell is fabricated and measured.
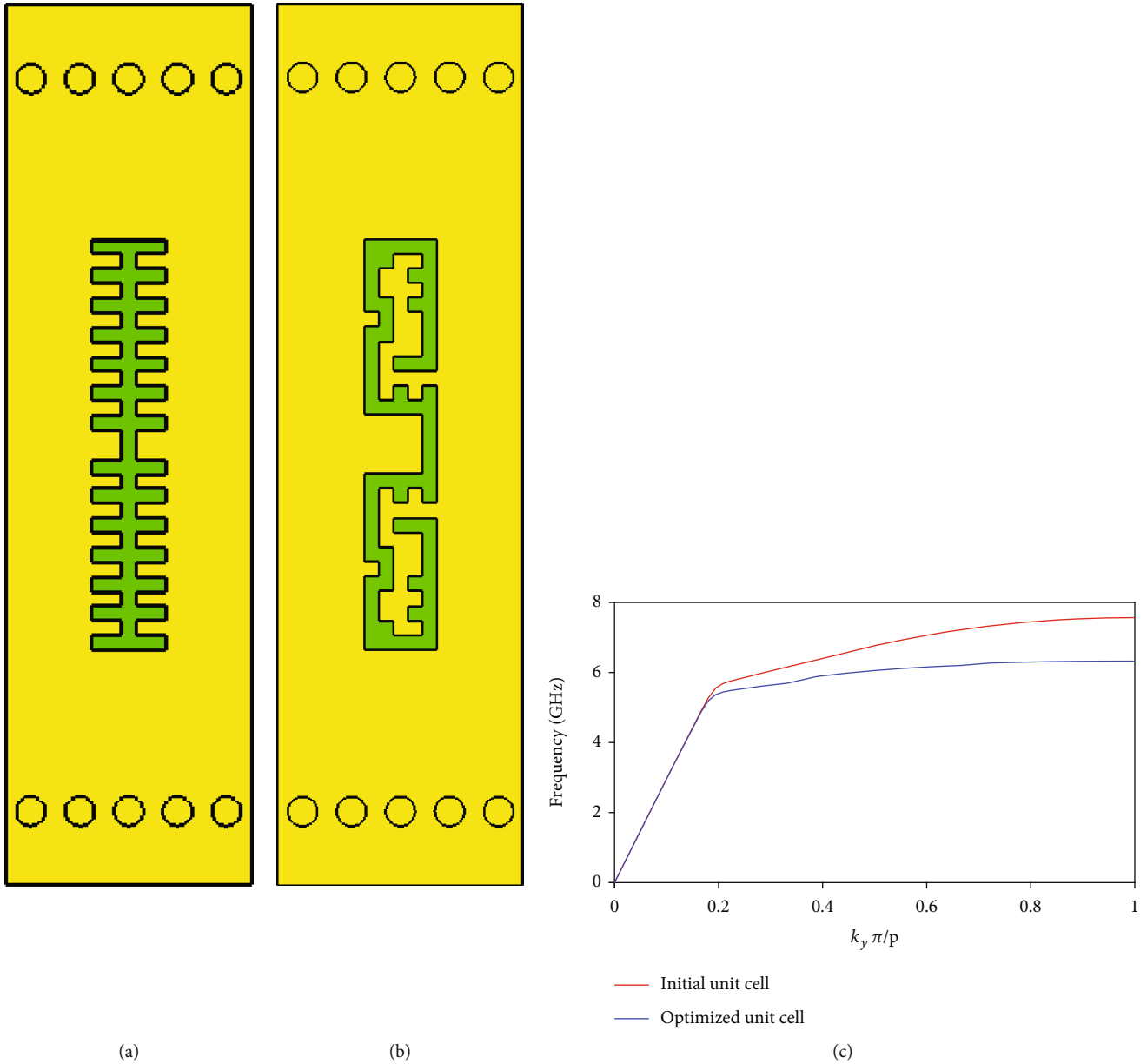
FIGURE 4: (a) Schematic configuration of the initial unit cell in the second design. (b) Schematic configuration of the optimized unit cell in the second design. (c) Dispersion curves of the unit cells in the second design. The parameters are selected as (in mm) $p = 5$, $p_x = p_y = 0.3$, $a = 15$, $w_s = 18$, $s = 1$, $S_x = 8.4$, and $S_y = 1.5$.

2. Unit Cell Design

The substrate is RO4003 with a thickness of 0.8 mm and a relative permittivity of 3.55. Figure 1 depicts a SIPW unit cell in which the location of the slot $(S_x \times S_y)$ is known, but its shape is unknown. To determine the slot shape, the location of the slot is pixelated as illustrated in Figure 1. Each pixel can be either "1" or "0" which corresponds to the absence or presence of the metal, respectively. In fact, each combination of binary values of pixels forms a binary matrix that is equivalent to a certain shape of the slot. Since the "0" or "1" status of each pixel affects the dispersion curve, by optimizing their different compositions, the desired dispersion curve can be achieved. In this paper, the

BPSO algorithm is applied to minimize the asymptotic frequency to a desired value. Among the various optimization methods with binary solution space, it has been shown that the BPSO method is much more efficient and has fewer parameters [20, 21]. It is also found that the BPSO algorithm converges faster than other algorithms because it is more targeted in each searching direction and avoids getting stuck in local optima [20, 22]. The BPSO algorithm has also been successfully used in pixelated structures [23–27]. The BPSO algorithm has a population (called a swarm) of candidate solutions (called particles) which move in the search space of the problem. The movement of particles in each iteration is based on the own best-known position and the swarm's best-known position. In each iteration of the optimization,

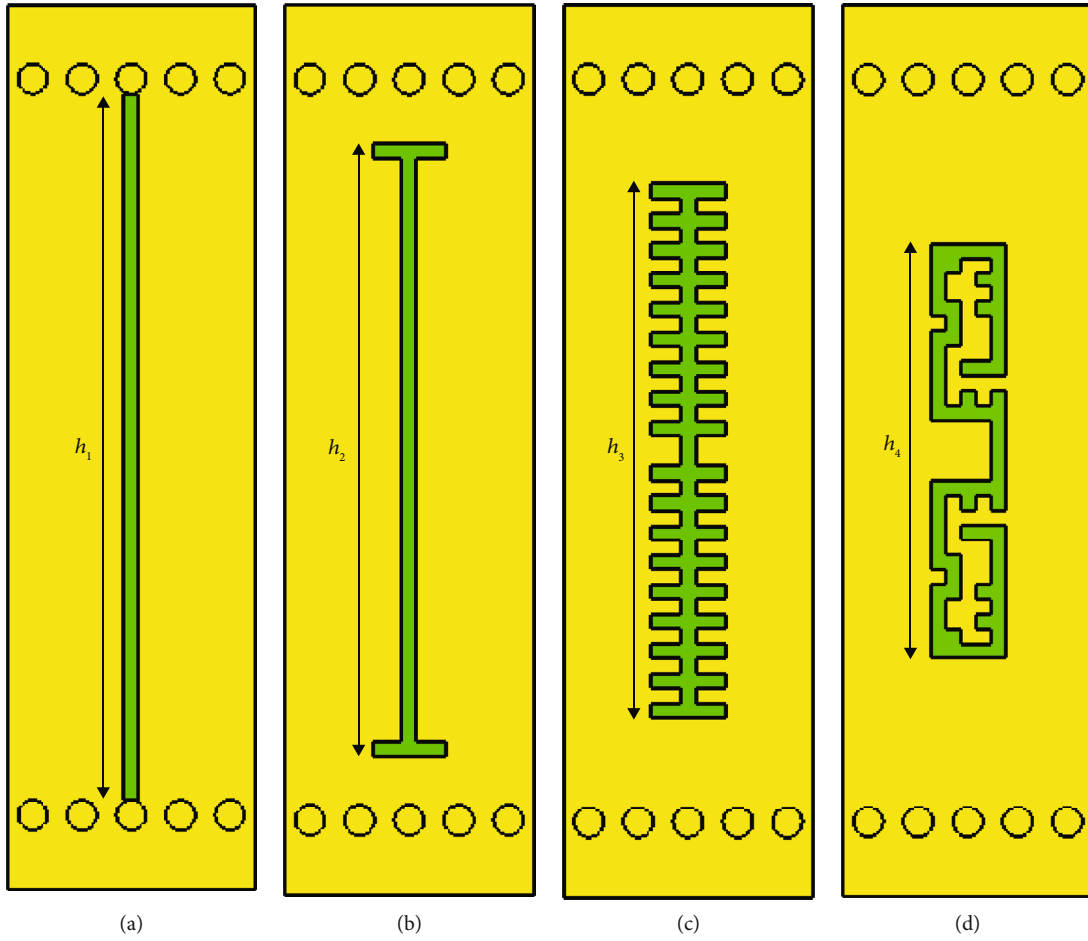FIGURE 5: Schematic configuration of the SIPW unit cells with (a) the rectangular-shaped slot, (b) T-shaped slot, (c) the Yagi-Uda antenna-like slot, and (d) the optimized slot; the parameters are (in mm) $h_1 = 14.4$, $h_2 = 12.4$, $h_3 = 10.8$, and $h_4 = 8.4$.
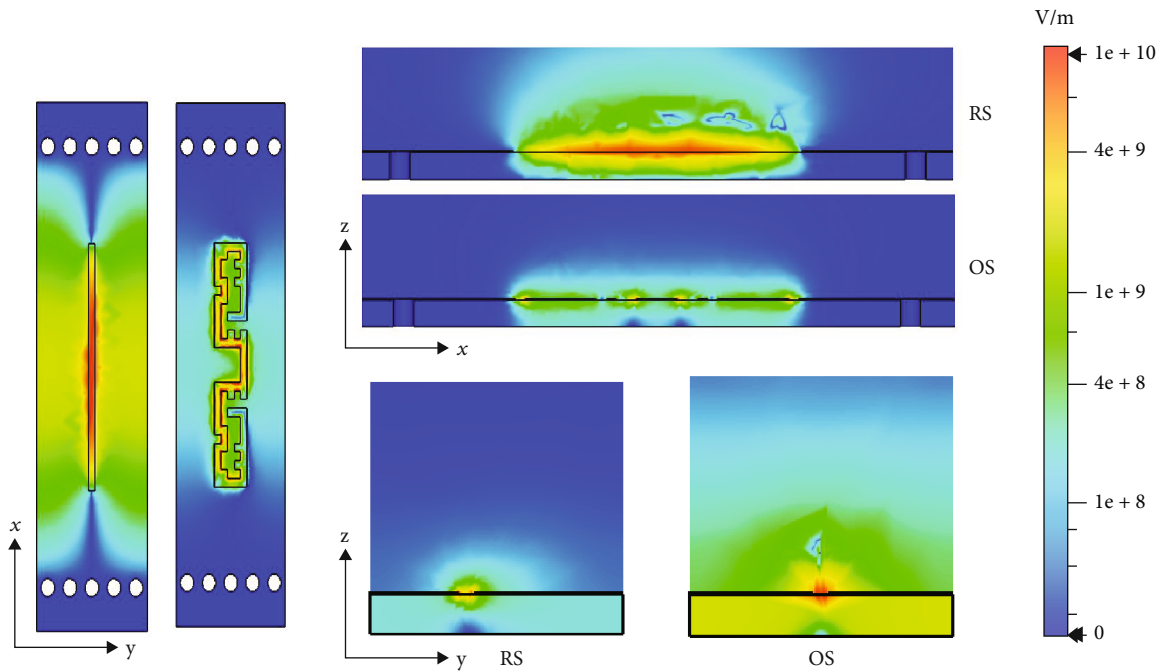

FIGURE 6: Simulated magnitude of electric field distribution for the unit cell with the rectangle-shaped slot (RS) and the optimized slot (OS).
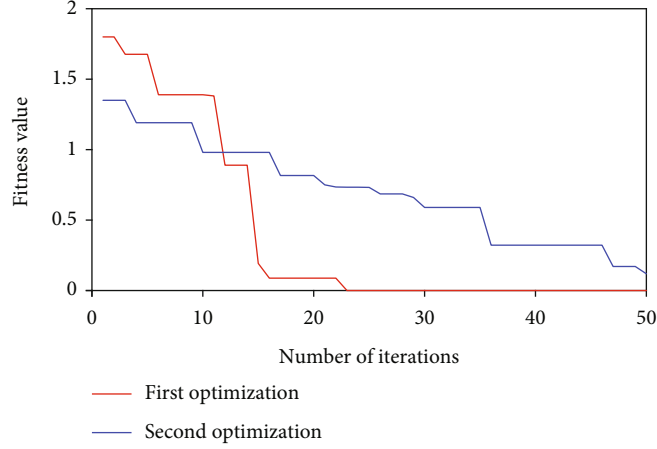
FIGURE 7: Convergence curve of the first and second optimization.

(a)

(b)
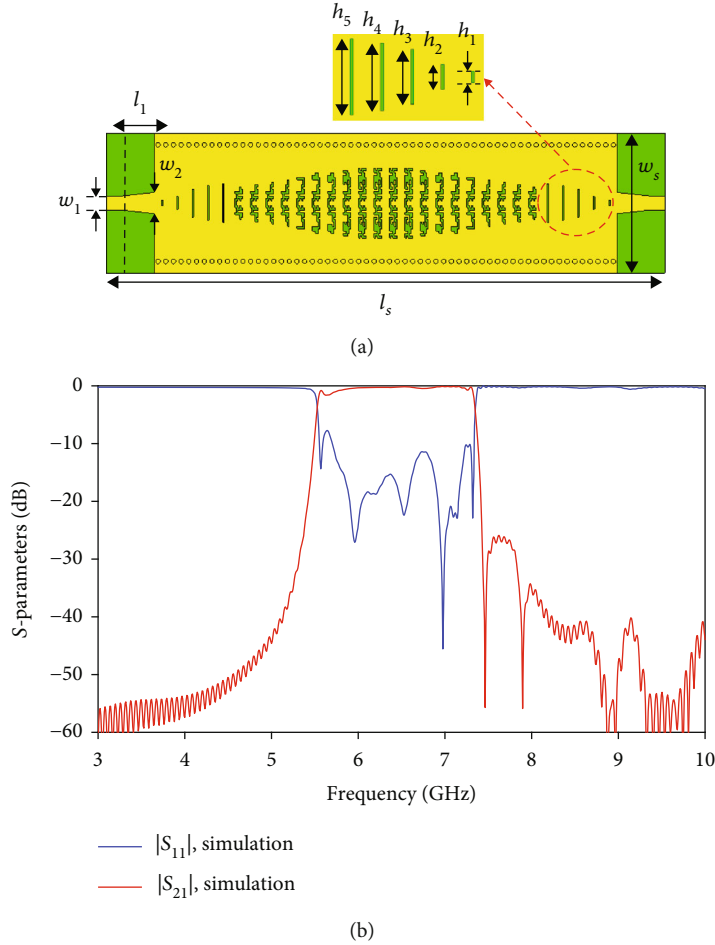
FIGURE 8: (a) Schematic configuration of the first proposed SIPW and (b) simulated S-parameters; the detail parameters are (in mm) $w_1 = 1.8$, $w_2 = 2.74$, $w_s = 18$, $l_1 = 4.2$, $l_s = 72.4$, $h_1 = 0.38$, $h_2 = 0.82$, $h_3 = 1.8$, $h_4 = 2.23$, and $h_5 = 2.5$.

the cost function of each particle is calculated using its dispersion curve obtained from the eigenmode solver of CST Microwave Studio (CST MWS). Therefore, it is necessary to appropriately link MATLAB (in which the optimization algorithm is written) and CST MWS. In addition, the initial solution can be selected from a unit cell that has already been proposed. The fitness function in the kth iteration of the optimization is defined as follows:

$$\text{fitness}^k = \max \left\{ f_{\max}^k - f_{\text{opt}}.0 \right\}, \tag{1}$$

(a)

(b)

(c)

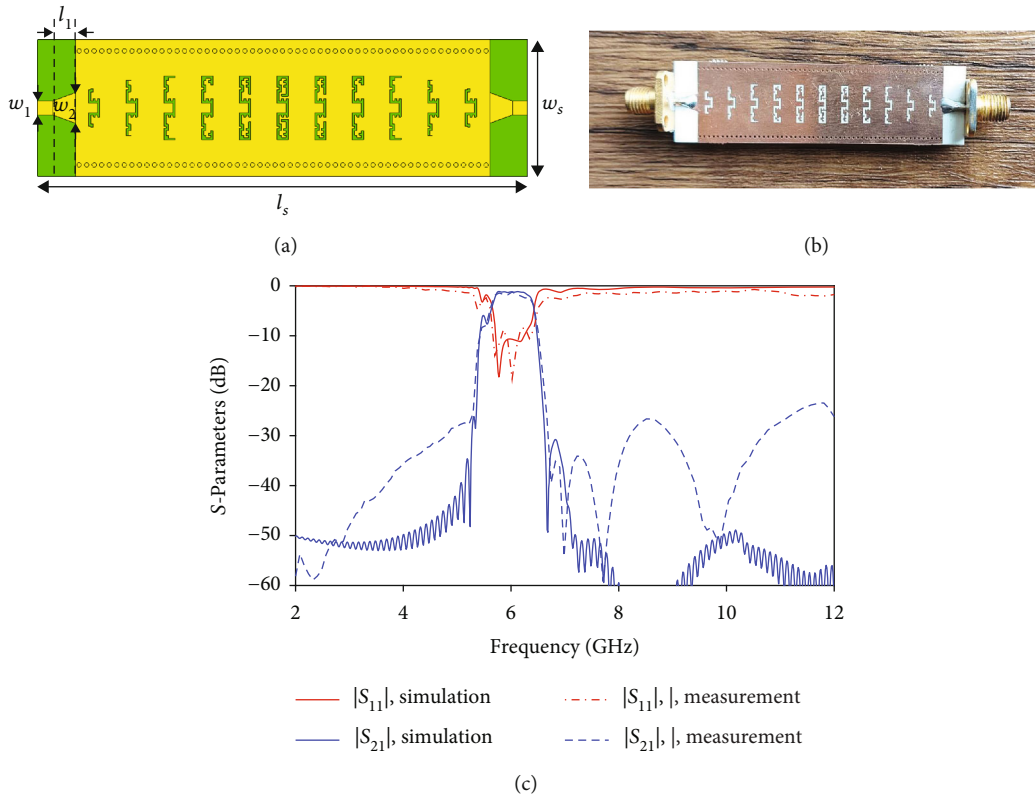FIGURE 9: (a) Schematic configuration of the second proposed SIPW, (b) fabrication prototype, and (c) simulated and measured S-parameters; the detail parameters are (in mm) $w_1 = 1.8$, $w_2 = 4$, $w_s = 18$, $l_1 = 3$, and $l_s = 65$.

where $f_{\max}^k$ is the maximum frequency of the dispersion curve in the kth iteration and f_{opt} is the desired maximum frequency under which we want the dispersion curve to be located. To increase the convergence rate, the number of pixels to be optimized can be reduced by considering two-fold symmetry with respect to the x-axis. It is clear that the low cut-off frequency depends only on the dimension of the SIW (especially the parameter of a) and cannot be changed with slot shape optimization. To clarify the optimization process, the flowchart of the program execution steps is shown in Figure 2. The main optimization program is implemented in MATLAB (green boxes), which is connected with CST to calculate the dispersion curves (blue box).

The design procedure has been examined with two examples. In the first design, we have considered the T-shaped slot as the initial solution. As shown in Figure 3, the asymptotic frequency of the T-shaped slot is about 8.8 GHz. The desired maximum frequency is also selected as 7 GHz. Concerning the symmetry of the slot shape, the dimensions of the half-shape binary matrix are 15×5. In the BPSO algorithm, the population size of particles is 20, and every particle includes 75 pixels to assign a pattern to the slot shape. After 23 iterations, the optimization process reaches the termination criteria, and the dispersion curve is placed under 7 GHz, as shown in Figure 3(c). The optimized shape of the slot is illustrated in Figure 3(b).

A Yagi-Uda antenna-like slot, shown in Figure 4(a), has been assumed as the initial guess in the second design.

According to our knowledge, this slot provides the lowest asymptotic frequency compared to the previous works. Its asymptotic frequency is obtained as 7.56 GHz with the dimensions mentioned in the caption of Figure 4. Note that the unit cell dimensions and pixelated region dimensions have changed with respect to the previous example. Considering bilateral symmetry, the number of pixels to be optimized in this example is 70, and the optimization parameters are the same as in the previous case. The desired maximum frequency is also supposed to be 6.2 GHz. The optimization is stopped after 50 iterations, and the asymptotic frequency reaches 6.3 GHz. The optimized shape of the unit cell and its dispersion curve are shown in Figure 4. It is clear that the optimized unit cell is more compact than the initial one. To visualize the compactness of the presented unit cell compared to the previous structures, Figure 5 shows the dimension of the slots in different unit cells which provide the same high cut-off frequency of 6.2 GHz. The length of the proposed slot reduces up to 42% compared with the length of the conventional rectangular-shaped slot. Based on the comparison between the unit cells of Figure 5, it is clear that to reduce the transverse frequency and concentrate more waves in the conventional unit cells, their dimensions should be larger. This causes the slots to be closer to the vias. Therefore, one should not expect suitable behavior from such a structure. In fact, instead of increasing the dimensions of the slots, we engineer them to reduce the transverse frequency.
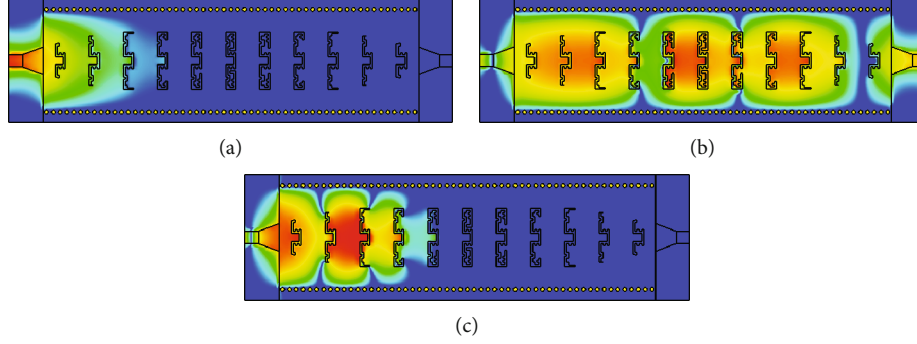
(a)

(b)

(c)

FIGURE 10: Simulated z-component of the electric field distribution of the second proposed SIPW waveguide at the frequency of (a) 4 GHz, (b) 6 GHz, and (c) 8 GHz.

TABLE 1: Comparison of the proposed filter with the state-of-the-art works.

Ref/shape of slot	Frequency (GHz)	Bandwidth (%)	$\|S_{21}\|$ (dB)	$\|S_{11}\|$ (dB)	Size/λ_g^2
[1] Rectangle-shaped slot	7.5-13	53	>-1	<-15	2.4×0.52
[12] Dumbbell-shaped slot	8-13.5	51	>-1	<-13	0.99×0.69
[14] T-shaped slot	5.6-7.3	26	>-1.83	<-10	0.86×0.43
[16] Yagi-Uda slot	13.5-18.4	30.7	>-2	<-10	0.8×0.42
[17] Meander slot	46.1-73.7	46	>-1.08	<-10	1.63×0.74
This work (second design)	5.6-6.3	11.7	>-2	<-10	0.82×0.22

To demonstrate the field confinement of the proposed unit cell, the electric field distributions of the unit cells with the conventional slot and the optimized slot having the same length are compared in Figure 6. It can be observed that the proposed structure demonstrates higher field concentration than that of the traditional unit cell.

Figure 7 displays the convergence curves of the BPSO algorithm in these two examples. The convergence rate of the second example is slower than that of the first example due to the compactness of its initial solution.

3. Simulation and Measurement Results

To verify the transmission characteristics of the proposed unit cells, in this section, two SIPW filters consisting of the proposed unit cells are designed. The configuration of the first one is depicted in Figure 8(a). The gradual matching technique of the transverse EM field to the transverse magnetic field is applied to the input and output of the structure. The simulated S-parameters are also shown in Figure 8(b). As predicted by the dispersion curve, this filter provides transmission between the frequencies of 5.6 GHz and 7.3 GHz. The configuration of the second one and its fabricated prototype are illustrated in Figures 9(a) and 9(b), respectively. As shown in Figure 9(c), the simulated and measured results, which are in good agreement, indicate transmission between 5.6 GHz and 6.3 GHz, which is consistent with the dispersion curve.

To get insight into propagation characteristics, the simulated electric field distributions of the second proposed structure at 4, 6, and 8 GHz are shown in Figure 10. At low and high stop bands, wave propagation is prohibited by SIW structure and slots, respectively. However, at the passband, the wave can effectively propagate through the structure and is highly localized.

In Table 1, the second designed filter is compared with similar structures in other references. All structures in this table are based on the combination of SIW and SSPP structures, whose low cut-off frequency is controlled by the width of the SIW waveguide and the high cut-off frequency is controlled by the SSPP slots. Since the bandwidth obtained in the proposed structure is less than that of other structures, the reduction of the high cut-off frequency by the slots is also greater in this structure. Also, the dimensions of this structure are smaller than others.

4. Conclusion

A novel and different procedure for the design of SIPW unit cells dependent on the dispersion curve optimization was proposed. Compared with the conventional design procedure, the SIPW unit cells designed with this procedure had high field confinement. To verify the proposed design, two unit cells with a miniaturized shape slot were designed which provided lower high cut-off frequencies than those of traditional unit cells. A 5.6-6.3 GHz bandpass filter with the proposed unit cell was fabricated. The measured results were in good agreement with the simulated ones. The method can be applied to the design of compact microwave and terahertz devices with adjustable bandwidths.

Data Availability

The data that support the findings of this study are available from the corresponding author upon reasonable request.

Conflicts of Interest

We have no conflicts of interest to disclose.

References

[1] L. Ye, Y. Chen, K. D. Xu, W. Li, Q. H. Liu, and Y. Zhang, "Substrate integrated plasmonic waveguide for microwave bandpass filter applications," *IEEE Access*, vol. 7, pp. 75957–75964, 2019.

[2] P. Chen, L. Li, K. Yang, and Q. Chen, "Hybrid spoof surface plasmon polariton and substrate integrated waveguide broadband bandpass filter with wide out-of-band rejection," *IEEE Microwave and Wireless Components Letters*, vol. 28, no. 11, pp. 984–986, 2018.

[3] L. Jidi, X. Cao, J. Gao, H. Yang, S. Li, and T. Li, "An ultrathin and compact band-pass filter based on spoof surface plasmon polaritons," *IEEE Access*, vol. 8, pp. 171416–171422, 2020.

[4] D. Zhang, K. Zhang, Q. Wu, and T. Jiang, "Efficient propagation of spoof surface plasmon polaritons supported by substrate integrated waveguide with bandpass features," *Journal of Physics D: Applied Physics*, vol. 53, no. 42, article 425104, 2020.

[5] S. D. Xu, D. F. Guan, Q. Zhang et al., "A wide-angle narrowband leaky-wave antenna based on substrate integrated waveguide-spoof surface plasmon polariton structure," *IEEE Antennas and Wireless Propagation Letters*, vol. 18, no. 7, pp. 1386–1389, 2019.

[6] S. Soleimani, S. Mirhadi, and N. Komjani, "Design of a broadband diplexer based on substrate integrated plasmonic waveguide," *International Journal of RF and Microwave Computer-Aided Engineering*, vol. 31, no. 11, article e22854, 2021.

[7] L. Liu, Z. B. Yang, D. F. Guan et al., "An SIW antenna utilizing odd-mode spoof surface plasmon polaritons for broadside radiation," *International Journal of RF and Microwave Computer-Aided Engineering*, vol. 30, no. 4, article e22177, 2020.

[8] B. Pan, P. Yu, Z. Liao, F. Zhu, and G. Q. Luo, "A compact filtering power divider based on spoof surface plasmon polaritons and substrate integrated waveguide," *IEEE Microwave and Wireless Components Letters*, vol. 32, no. 2, pp. 101–104, 2022.

[9] Z. Chen, M. Wang, D. Guan, Z. Qian, W. Wu, and L. Zhu, "Wideband filtering antenna fed through hybrid substrate integrated waveguide and spoof localized surface plasmon structure," *IEEE Transactions on Antennas and Propagation*, vol. 70, no. 5, pp. 3812–3817, 2022.

[10] S. D. Xu, L. Liu, D. F. Guan et al., "A hybrid substrate integrated waveguide and spoof surface plasmon polaritonleakywaveantenna with open stopband suppressed," *International Journal of RF and Microwave Computer-Aided Engineering*, vol. 32, no. 11, Article ID e22413, 2022.

[11] S. Wang, K. Chung, F. Kong, L. Du, and K. Li, "A unidirectional frequency beam-scanning antenna using composite slow-wave waveguide based on substrate integrated waveguide and spoof surface plasmon polariton structure," *IET Microwaves, Antennas & Propagation*, vol. 15, no. 14, pp. 1833–1841, 2021.

[12] R. S. Sangam and R. S. Kshetrimayun, "Hybrid spoof surface plasmon polariton and substrate integrated waveguide bandpass filter with high out-of-band rejection for X-band applications," *IET Microwaves, Antennas & Propagation*, vol. 15, no. 3, pp. 289–299, 2021.

[13] X. Wang, Y. Li, H. Li, and W. Wu, "Broadband filtering balun employing spoof surface plasmon polariton and substrate integrated waveguide," *AEU - International Journal of Electronics and Communications*, vol. 160, article 154511, 2023.

[14] P. Chen, L. Li, K. Yang, and F. Hua, "Design of substrate integrated plasmonicwaveguide bandpass filter with T-shaped spoof surface plasmon polaritons," *Electromagnetics*, vol. 40, no. 8, pp. 563–575, 2020.

[15] B. Zhang, Z. Li, M. Wang et al., "Narrowband SIW-SSPP hybrid bandpass filter with compact profile at Ka-band," *IEEE Access*, vol. 11, pp. 98305–98314, 2023.

[16] H. Zhu, Y. Zhang, L. Ye, Y. Li, Y. Xu, and R. Xu, "On-chip terahertz bandpass filter based on substrate integrated plasmonic waveguide," *Results in Physics*, vol. 27, article 104553, 2021.

[17] D. Pan, B. You, X. Wen, and X. Li, "Wideband substrate integrated waveguide chip filter using spoof surface plasmon polariton," *Micromachines*, vol. 13, no. 8, p. 1195, 2022.

[18] Y. Luo, J. Yu, Y. Cheng, F. Chen, and H. Luo, "A compact microwave bandpass filter based on spoof surface plasmon polariton and substrate integrated plasmonic waveguide structures," *Applied Physics A: Material Science & Processing*, vol. 128, no. 2, 2022.

[19] Z.-M. Wu, L. Ji, H.-B. Zhu, and J.-F. Mao, "A slow wave folded ridge HMSIW using spoof surface plasmon polaritons structure and its application in coupler design," *IEEE Transactions on Components, Packaging and Manufacturing Technology*, vol. 13, no. 5, pp. 594–603, 2023.

[20] X. Ju, G. Zhu, F. Huang et al., "Reverse design of pixel-type terahertz band-pass filters," *Optic Express*, vol. 30, no. 2, pp. 957–965, 2022.

[21] F. Grimaccia, M. Mussetta, A. Niccolai, and R. E. Zich, "Comparison of binary evolutionary algorithms for optimization of thinned array antennas," in *2018 IEEE Congress on Evolutionary Computation (CEC)*, Rio de Janeiro, Brazil, 2018.

[22] T. M. Shami, A. A. El-Saleh, M. Alswaitti, Q. Al-Tashi, M. A. Summakieh, and S. Mirjalili, "Particle swarm optimization: a comprehensive survey," *IEEE Access*, vol. 10, pp. 10031–10061, 2022.

[23] S. Mirhadi and M. Soleimani, "Topology design of dual-band antennas using binary particle swarm optimization and discrete Green's functions," *Electromagnetics*, vol. 35, no. 6, pp. 393–403, 2015.

[24] S. Mirhadi, N. Komjani, and M. Soleimani, "Ultra wideband antenna design using discrete Green's functions in conjunction with binary particle swarm optimisation," *IET Microwaves, Antennas & Propagation*, vol. 10, no. 2, pp. 184–192, 2016.

[25] B. Ghaderi, V. Nayyeri, M. Soleimani, and O. M. Ramahi, "Pixelated metasurface for dual-band and multi-polarization electromagnetic energy harvesting," *Scientific Reports*, vol. 8, no. 1, article 13227, 2018.

[26] M. Borgese, F. Costa, S. Genovesi, A. Monorchio, and M. Giuliano, "Optimal design of miniaturized reflecting meta-surfaces for ultra-wideband and angularly stable polarization conversion," *Scientific Reports*, vol. 8, no. 1, p. 7651, 2018.

[27] M. Ullah, R. Keshavarz, M. Abolhasan, J. Lipman, and N. Shariati, "Low-profile dual-band pixelated defected ground antenna for multistandard IoT devices," *Scientific Reports*, vol. 12, no. 1, article 11479, 2022.